Article

Journal of the Brazilian Chemical Society

https://dx.doi.org/10.21577/0103-5053.20240063

J. Braz. Chem. Soc. **2024**, *35*, 11, e-20240063, 1-8

Functionalized Crumpled Graphene as Nanocatalysts for Organophosphate Neutralization

Yane H. Santos,[a] Leandro Hostert,[a,b] Thiago S. D. Almeida,[a,c] Aldo J. G. Zarbin,[a] Victor H. R. Souza[c] and Elisa S. Orth[*,a]*

[a]*Departamento de Química, Universidade Federal do Paraná (UFPR), 81531-990 Curitiba-PR, Brazil*

[b]*Departamento de Engenharia, Física e Matemática, Instituto de Química, Universidade Estadual Paulista (UNESP), 14800-060 Araraquara-SP, Brazil*

[c]*Faculdade de Ciências Exatas e Tecnologia, Universidade Federal da Grande Dourados (UFGD), 79804-970 Dourados-MS, Brazil*

Organophosphates are prevalent in agrochemicals and chemical warfare agents, posing significant health and safety concerns. These compounds are known for their high chemical stability and to address this issue, nucleophilic catalysts have emerged as a promising solution for their degradation. Herein, we focus on a novel material created through the combined effects of imidazole and crumpled graphene (CG) to develop a nanocatalyst for the neutralization (i.e., degradation) of organophosphates (OPs). The strategy involves the covalent functionalization of CG with imidazole groups without disrupting the three-dimensional structure of CG. This unique combination results in a synergistic effect between neighboring imidazole groups within CG, significantly enhancing the catalytic performance. The catalytic increment (k_{CAT}/k_{H2O}) achieved is in the order of 10^4, demonstrating the remarkable efficiency of this catalyst. The pioneering and promising use of functionalized CG for addressing concerns with chemical security can boost and be broadened to other applications.

Keywords: organophosphates, nucleophilic nanocatalyst, imidazole, functionalized crumpled graphene (CG), chemical security

Introduction

The organophosphate class is on the worldwide radar regarding health and safety concerns since they are present in many agrochemicals and chemical warfare.[1-4] Hence, developing fast and effective procedures to neutralize (i.e., degrade or detoxify) them has been interesting. These neutralization reactions can be used to eliminate undesired stocks and also for their detection to alert improper use or chemical attacks.[5] Organophosphates are known for their high chemical stability with half-life times ($t_{1/2}$) exceeding the human being lifetime,[6] thus one of the most promising ways to degrade them is to use nucleophilic catalysts.[7,8]

Imidazole is a promising catalytic group for neutralizing organophosphates due to its presence in enzymatic sites responsible for vital dephosphorylation processes.[9-13] Furthermore, imidazole has a broad catalytic behavior due to its versatile roles as base, acid, and nucleophile.[14] The use of bare imidazole to degrade organophosphates is well known, and its mechanisms of action are already very well described.[1] However, these homogeneous catalysts have drawbacks, such as recovery and recycling, when projecting real-life applications for neutralizing or detecting toxic agents. An option to deal with this problem is to mimic the enzymatic sites using the imidazole anchored in different backbones, furnishing heterogeneous catalysts with possible synergistic effects. Successful examples use polymers,[15,16] cellulosic residues (rice husk),[17] and carbonaceous nanostructures[18] (graphene/graphene oxide and carbon nanotube), among others.[19-21] These supports are covalently functionalized with imidazole derivatives seeking synergy, greater stability, easier handling, and higher catalytic activity and, therefore, better performance in neutralizing toxic organophosphates. Numerous combinations of catalysts for degradation have been studied; among them,

*e-mail: elisaorth@ufpr.br
Editor handled this article: Célia M. Ronconi (Associate)

2D materials, in particular graphene oxide, have received significant attention in recent years due to their excellent properties as support: excellent electronic properties, facile functionalization sites (especially the oxygenated groups), mechanical resistance, among others.[22-26]

Graphene, as a catalyst supports for organophosphate degradation, has a favorable history of catalytic improvement. Many chemical groups with known catalytic activity have been evaluated, such as imidazole,[18] hydroxamic acid[27] and thiol.[28] In most cases, the synthetic route results in 2D-modified graphene, where the catalytic improvement arises from cooperative effects. Despite the excellent properties of 2D graphene-based composites, better catalytic performance can be compromised due to the stacking of graphene sheets as a consequence of strong van der Waals interaction.[29] Crumpling the 2D structures of graphene into 3D paper ball-like structures, the so-called crumpled graphene (CG), throughout a spray pyrolysis approach has been demonstrated as a clever way to maintain the intrinsic characteristics of 2D graphene, combined with 3D characteristics, such as porosity, high specific surface area, and mechanical properties.[30-33] This material has proven an interesting alternative for graphene modifications in applications such as supercapacitors[34-37] and gas sensing,[38] electrochemical sensors[39,40] and batteries.[41,42] Additionally, the remaining functional groups over the CG may serve as a targeting site for covalent modification, becoming an approach for designing new graphene-based materials with improved catalytic performance.[43,44]

Herein, we report the covalent functionalization of CG with imidazole groups for organophosphate degradation. We synthesized bare CG structures using aerosol-assisted capillary compression followed by covalent functionalization on the carboxylic acid groups. Allying the potentialities of CG and imidazole, we investigated the influence of the morphological structure of the substrate both in the functionalization process and in the detoxification reactions of organophosphate as the possible synergistic effects between imidazole and other neighboring groups on CG. To the best of our knowledge, this is the first report of CG functionalization for catalytic application in the neutralization of organophosphates.

Experimental

Materials and methods

Graphite was purchased from the National Graphite Company (Itapecerica, Brazil) (graflake 99580) with a purity of 99.84%.[45] Other reactants were purchased from Sigma-Aldrich (Steinheim, Germany) and used without any purification. The organophosphate diethyl 2,4-dinitrophenyl phosphate (DEDNPP) was obtained according to the method previously reported.[46]

CG synthesis

Crumpled graphene was synthesized[30,31] from graphene oxide (GO) previously prepared using a modified Hummers method.[35] Briefly, 1 mg mL^{-1} of a GO dispersion was nebulized into a tubular furnace preheated at 300 °C using a nitrogen gas flow of 1 L min^{-1}. Next, the CG sample was collected using a polytetrafluoroethylene membrane adapted at the exhaust. The sample was washed and centrifuged 3-fold with water, followed by acetone. Finally, the CG was dried at 60 °C for 30 min before the next steps.

Functionalization of CG

The procedure to synthesize CG functionalized with imidazole groups, CGIMZ composite is summarized in Scheme 1. Shortly, *N*-hydroxysuccinimide (NHS, 0.68 g, 5.91 mmol) and 1-ethyl-3-(3-dimethylaminopropyl) carbodiimide (EDC, 1.14 g, 5.94 mmol) were added into 20 mL of 1.0 mg mL^{-1} CG dispersion.[18] The dispersion was stirred for 1 h at low temperature (ca. 0 °C) and 1 h at room temperature (ca. 23 °C). Then, 376 µL (3 mmol) of 1-(3-aminopropyl)imidazole (API) was added, leading to the nanomaterial CGIMZ.[18] The product (CGIMZ) was separated by filtration, washed with Milli-Q water, and dried at 50 °C.

Characterization

Using the attenuated total reflection (ATR) method, Fourier transform infrared spectroscopy (FTIR) was carried out on a Bruker INVENIO-R spectrophotometer (Bruker, Ettlingen, Germany) over the 4000-400 cm^{-1}. Thermogravimetric analysis (TGA) was carried out in a SDT Q600 equipment (TA Instruments, New Castle, USA) under an air atmosphere (100 mL min^{-1}), at a heating rate of 5 °C min^{-1}, from 30 to 1000 °C. Scanning electron microscopy (SEM) analysis was obtained using a Tescan SEM (Tescan, Brno, Czech Republic) by deposition of CG and CGIMZ dispersed in isopropanol onto a silicon substrate.

Kinetics

Catalytic studies were performed using the organophosphate DEDNPP and were analyzed by UV-Vis spectroscopy in Agilent model Cary 60 UV-Vis spectrophotometer (Santa Clara, USA). CGIMZ was added

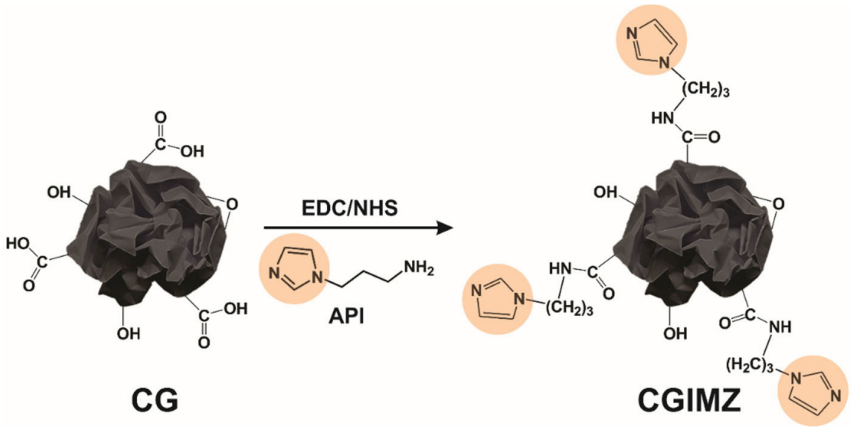

Scheme 1. Overview of the chemical functionalization of CG.

in a quartz cuvette containing 3 mL of 0.01 mol L^{-1} buffered solution of $KHCO_3$ (pH 8.5). The reaction started with the addition of 10 µL of a solution of DEDNPP (6×10^{-3} mol L^{-1} in acetonitrile), which was kept at a temperature of 23 °C and stirring of 1000 rpm. Periodically, agitation was paused, and the absorbance of the solution was measured by UV-Vis spectra. The organophosphate degradation was measured by the absorbance variation in 400 nm related to the product 2,4-dinitrophenol (DNP). Rate constants were obtained by fitting with pseudo-first-order kinetics.[17] The constants are presented in $min^{-1}g^{-1}$ obtained by the ratio between the pseudo-first-order constant and the total mass used by the nanocatalyst, facilitating comparison.

Results and Discussion

Herein, the chemical modification on the CG surface with imidazole was based on a previous functionalization performed with GO, benefiting from the oxygenated groups on the surface of these carbon nanostructures.[18,46,47] As well as GO, the CG nanomaterial presents abundant oxygenated functional groups, enabling similar functionalization approaches. In this case, the functionalization route at the carboxylic acid sites of CG benefits from the activation agents EDC/NHS and an amine terminal reagent (containing imidazole groups also). This amine couples to the carboxylic acid, leading to an amide bond with the CG surface and enables freely available imidazole groups to be an anchored by this means. This amide bond is known to be stable and resistant towards hydrolysis.[18,46,47] The functionalized nanomaterial (CGIMZ) was applied as a nanocatalyst in the detoxification reaction of the organophosphate DEDNPP.

Characterization

The FTIR spectra in Figure 1a exhibit the first indications of successful functionalization by comparing the bands of the non-functionalized CG and the functionalized CGIMZ. The infrared analysis confirmed bands formed after functionalization reactions (e.g., amide bond). For CG, bands of stretching and deformation modes of the oxygenated groups are observed. These bands are the result of the graphite oxidation process and refer to the oxygenated functional groups of carboxylic acids, hydroxyls, epoxides, and ketones: 3320 cm^{-1} O–H hydroxyls stretching, 1714 cm^{-1} C=O carboxylic acids stretching, 1573 cm^{-1} C=OH group, 1229 cm^{-1} C–O–C epoxides, and 1046 cm^{-1} C–O alkoxy.[48-50]

Upon functionalization, the decrease in the intensity of some bands of oxygenated groups, such as the O–H band (3290 cm^{-1}) and the C=O band of carboxylic acids (1726 cm^{-1}), is the first indication of CG covalent modification. In addition, new bands referring to amide bonds indicate functionalization, such as the N–H flexion (3290 cm^{-1}), C–N uncoupled (1555 cm^{-1}), and C=O stretching amides (1635 cm^{-1}) bands. Bands of the imidazole ring, such as C–N stretching in 1358 and 1438 cm^{-1}, were also depicted.[46,51] Overall, FTIR can confirm that covalent functionalization occurred through the terminal amine group of imidazole attached to CG, which can be seen by the presence of the mentioned bands.

Regarding the TGA analysis (Figure 1b), it is possible to confirm the functionalization and indicate its degree. For the non-functionalized material (CG), two mass loss events are observed: (*i*) a first event ranging from 70 to 300 °C, corresponding to oxygenated groups of the CG structure (19.5%), and (*ii*) second event ranging from 350 to 500 °C, related to pyrolysis of the CG carbon structure (65.7%). After functionalization, in addition to the losses associated with oxygenated groups (10.9%) and pyrolysis of the carbon structure (55.4%), there is a mass loss of around 250-400 °C, related to functionalized groups on the surface of the CG. The value of this mass loss event

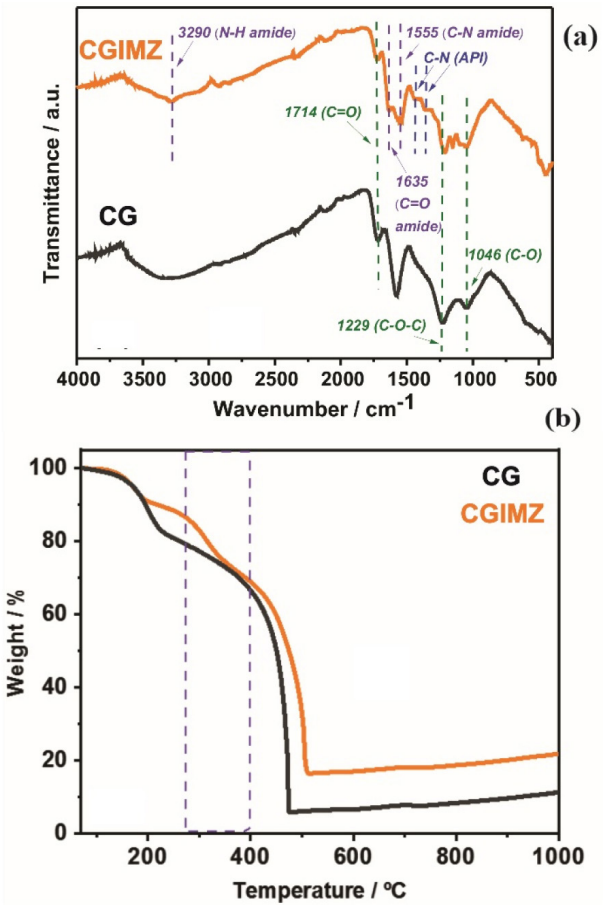

Figure 1. FTIR-ATR spectra (a), and TGA curves (b) for CG and CGIMZ.

referring to the CGIMZ is 22%. Also, a decrease in the percentage referring to events of mass loss of oxygenated groups (70-300 °C) after functionalization is noticed, from 19.5 in CG to 10.9% for CGIMZ. The decrease in oxygenated groups in CGIMZ agrees with the functionalization of the covalent-modified CG.

Morphological results based on SEM analysis are shown in Figure 2. The method of spraying a graphene oxide dispersion into the heated zone at 300 °C successfully produces crumpled graphene.[35,39] Crumpled graphene ball-like structures resulting from the isotropic compression of graphene oxide droplets are observed in Figures 2a and 2b. Throughout this process, when the water droplets face a high-temperature environment at the tubular furnace, they go from liquid to gas phase, and the graphene oxide sheets into those droplets are compressed in crumpled graphene, concomitantly its thermal reduction.[30,31] The presence of ridges and vertices is noticed in all materials.[52] The paper ball-like morphology of the crumpled graphene is preserved after functionalization with API, as depicted in Figures 2c and 2d. This is expected as seen in other related studies with covalent functionalization with GO and carbon nanotubes.[18,27,28,53] In fact, the low degree of functionalization guarantees that the precursor properties are maintained so its morphology is not expected to significantly change. Nitrogen atoms on the CG surface (around 8.8%) are also confirmed throughout the energy dispersive X-ray spectroscopy (EDS) spectra in Figure 2e. No peak corresponding to nitrogen atoms is noticed for the CG sample. Meanwhile, a contribution of nitrogen is seen for CGIMZ, agreeing with vibrational and thermal results.

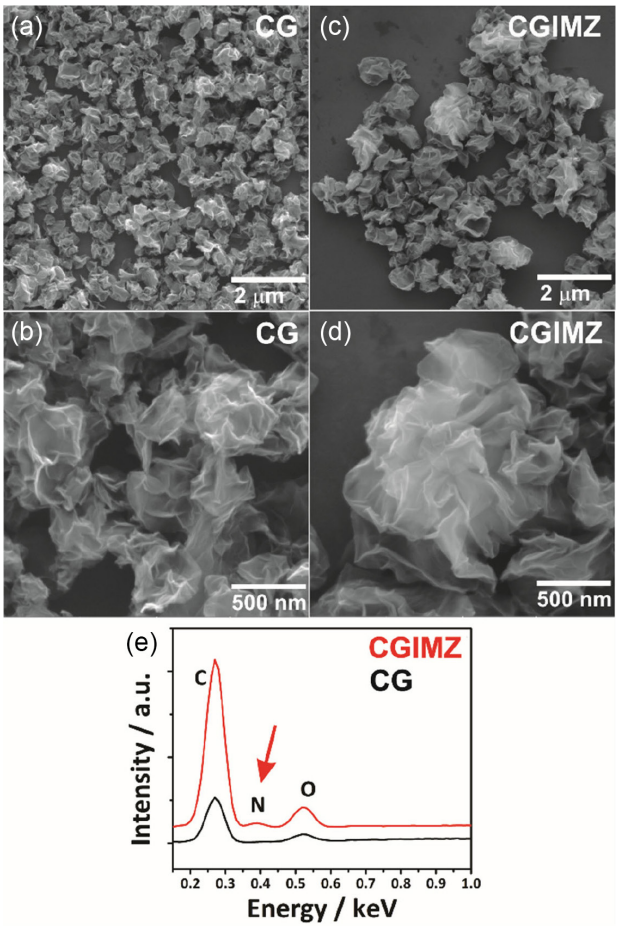

Figure 2. SEM images for bare CG (a-b) and CGIMZ (c-d); EDS spectra (e) of CG (black line) and CGIMZ (red line).

Catalytic studies

The functionalized nanomaterial (CGIMZ) was applied as a heterogeneous nanocatalyst for the dephosphorylation reaction with the pesticide simulant DEDNPP. The presence of the imidazole group is known to have efficient activity in the detoxification of organophosphates. The DEDNPP degradation reaction is shown in Figure 3.

The confirmation of the degradation of DEDNPP is accompanied by UV-Vis spectroscopy due to the formation of the product DNP (Figure 4a), which illustrates the DEDNPP reaction spectrum in the presence of CGIMZ. The spectra were verified before and after the reaction studies,

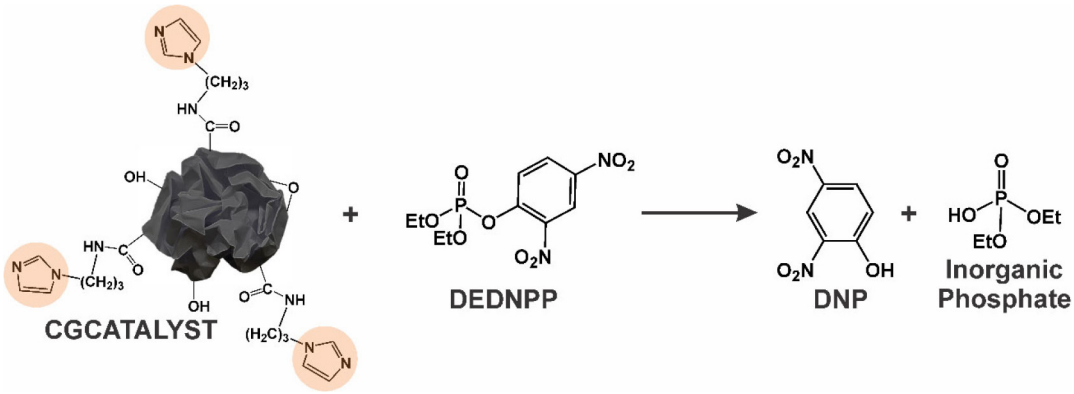

Figure 3. Degradation reaction of DEDNPP in the presence of the nanocatalyst.

showing a decrease in the band at 250 nm referring to the reagent (DEDNPP) and an increase at 400 nm referring to the product (DNP). The illustration of the reaction medium before and after was also presented (inset in Figure 4a), in which, initially, it is a colorless suspension. After the formation of the reaction product, there is a change in the color to yellow color. As for the relationship between the band intensity at 400 nm and time, it was possible to obtain a characteristic pseudo-first-order kinetic profile (Figure 4b).

For non-functionalized CG, the rate constant was comparable to the spontaneous reaction, hence did not show any significant activity, which is expected due to the absence of strong nucleophilic groups. For functionalized CGIMZ, the rate constant of 1.41 min^{-1} g^{-1} was obtained. This means that the reaction that would take 15 days in the absence of a catalyst, would take under 3 min (considering 1 g of nanocatalyst).[47] The increase in catalytic activity, when compared to non-functionalized CG, was attributed to the nucleophilic imidazole groups anchored on the CG surface. Compared with bare API (0.26 min^{-1} g^{-1}),[53] the performance of CGIMZ is significantly better, indicating strong synergistic effects by the CG surface. Moreover, it is possible to compare to other imidazole-derived GO nanocatalysts reported previously.[47] Namely, GO was monfunctionalized GO on the carboxylic sites with API giving GOIMZ. Also, GO was bifunctionalized on the carboxylic site with API and thiol derivative, giving GOSHIMZ. Rate constants of 0.54 and 0.62 min^{-1} g^{-1} were obtained for GOIMZ and GOSHIMZ, respectively.[47] The higher activity for CGIMZ evidences the potential of using CG as a precursor for nanocatalysis.

It is also possible to evaluate the performance of the nanocatalysts from the catalytic increment (k_{CAT}/k_{H2O}), which was obtained by comparing the constant of the DEDNPP spontaneous hydrolysis reaction (k_{H2O}) with the catalytic constant (k_{CAT}).[17] For CGIMZ, rate enhancements of 1 × 10^4-fold, are among the highest reported in the literature. For GOIMZ and GOSHIMZ (from previous studies)[47] these values range in the order of 10^3-fold. Such a result indicates that the morphology of the precursor of the nanocatalyst (in this case, the CG) influences the catalytic performance since the degree of functionalization is not greatly different. The CGIMZ outstands even the bifunctionalized nanomaterial GOSHIMZ, which has two different nucleophilic groups (thiol and imidazole

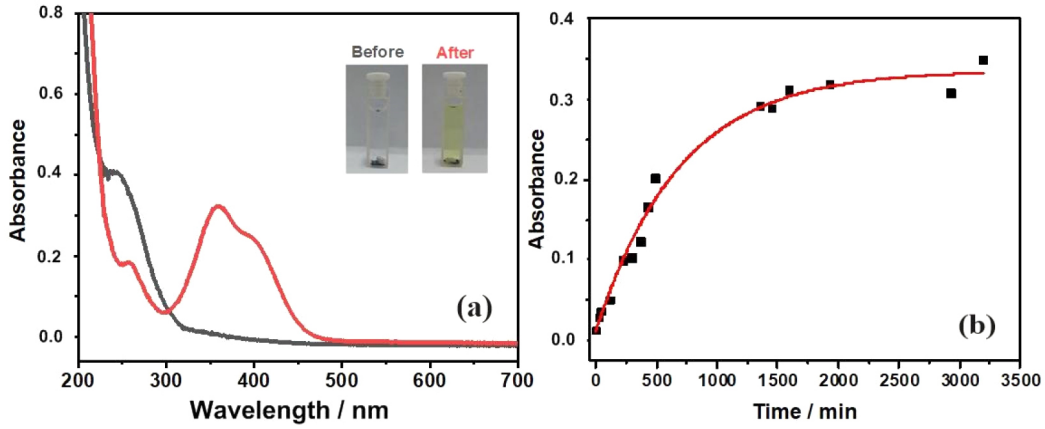

Figure 4. (a) Spectra and photographs (inset) before (black line) and after (red line) the DEDNPP dephosphorylation reaction (6 × 10^{-5} mol L^{-1}, pH 8.5). (b) Kinetic profile at 400 nm for the reaction of DEDNPP with CGIMZ fitted with pseudo-first order equation.

group) which present better catalytic properties than the analogue monofunctionalized (GOIMZ).[47] This shows that the carbonaceous matrix has a significant influence on the catalysis. The superiority in catalysis concerning other functionalized nanomaterials may be related to the synergism between the crumpled morphology, availability of the imidazole groups anchored, and also to additional cooperative effects such as general base catalysis by neighboring oxygenated groups.[47]

The proposed mechanism for the action of CGIMZ in the neutralization reaction of DEDNPP is shown in Figure 5. Firstly, a favorable attraction of the organophosphate on the CGIMZ backbone can be favored (i.e., by van der Waals interactions), positioning it nearer to the imidazole active groups. This attraction and better interaction may also be related to the greater surface area of CG compared to GO. Therefore, this first attraction/adsorption step is essential for the exceptional performance of functionalized CG as a catalyst.[54-56] Then, the imidazole group on CGIMZ attacks the phosphorus electrophilic center of DEDNPP, with the cleavage of the P–O bond. This leads to the phenolic product DNP and a phosphorylated intermediate, which is subsequently hydrolyzed, generating the final phosphoric acid derivative (less toxic) and thus recycling the nanocatalyst.[18] This mechanism has been widely accepted for imidazole-derived catalysts based on thorough mechanistic studies (theoretical, mass spectroscopy, nuclear magnetic resonance spectroscopy).[1] Indeed, the recovery and recycling of imidazole-based catalysts have been proven and widely known.[1,47] Therefore, we expect that the nanocatalyst CGIMZ can be recycled, recovered and reused several cycles without losing activity.[46] Indeed, related studies do not indicate any kind of poisoning or other pathways that could affect the reactivity of the catalysts. Further studies will be carried out to confirm the recycling feature.

From the catalytic study, the functionalized CGIMZ has a high potential for organophosphate neutralization. This is the first work that explores the targeted functionalization of CG for catalytic purposes in organophosphate reactions. The novelty of functionalization for this type of nanomaterial opens up space for several other modification possibilities (different from nanocomposites) since the targeted functionalization is an interesting tool for improving or adding properties to the nanomaterial.

Conclusions

Overall, this study introduces a novel nanomaterial, CGIMZ, that demonstrates exceptional promise in nanocatalysis. By targeting the functionalization of CG with imidazole groups, a unique 3D configuration should account for the better performance of CG, in contrast to GO-based materials. Indeed, CGs are known to have higher surface area, facilitating increased functional group accessibility and enhancing catalytic performance. The potential of CGIMZ as an efficient nanocatalyst for organophosphate detoxification is evident.

Importantly, these results mark a pioneering step in the targeted functionalization of CG for organophosphate detoxification, opening up new possibilities for modifying CG-based nanomaterials to potentiate their catalytic properties. CGIMZ represents a promising advancement in nanocatalysis, offering innovative solutions for addressing environmental and health challenges associated with organophosphate pollutants. In this sense, contributing

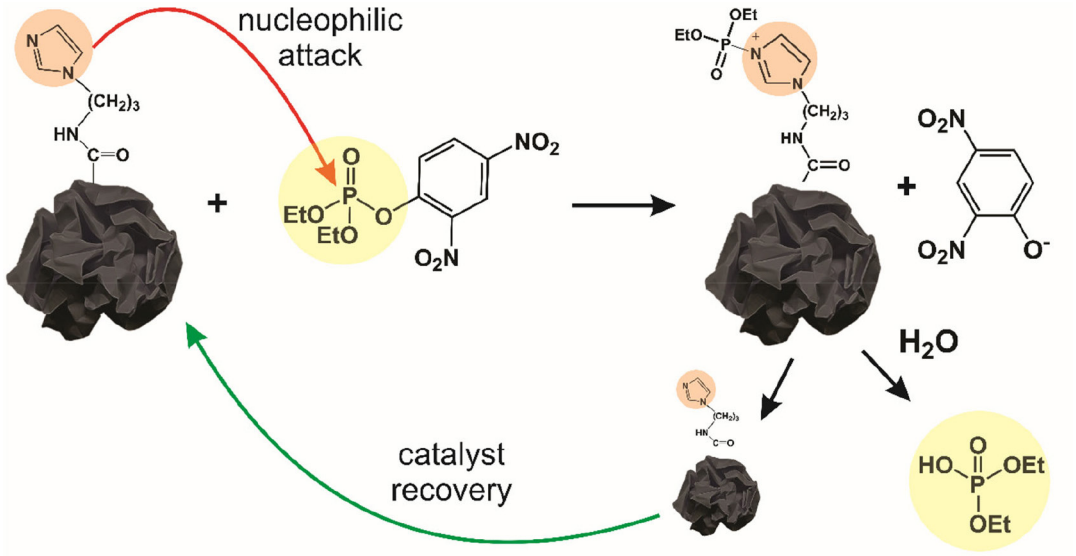

Figure 5. Proposed mechanism for the reaction of CGIMZ with DEDNPP.

to the promotion of chemical security and safety, is a worldwide concern.

Acknowledgments

This work was supported by UFPR, CNPq, CAPES, L'Oréal-UNESCO-ABC, PhosAgro/UNESCO/IUPAC, National Institute of Science and Technology of Nanomaterials for Life (INCTNanovida), National Institute of Science and Technology of Carbon Nanomaterials (INCTNanocarbon) and Academic Cooperation Program in Public Security and Forensic Sciences-CAPES.

Author Contributions

Yane H. Santos was responsible for data curation, validation, visualization, writing (original draft, review and editing); Leandro Hostert for data curation, validation, visualization, writing (original draft, review and editing); Thiago S. D. Almeida for data curation, validation, visualization, writing (original draft, review and editing); Aldo J. G. Zarbin for conceptualization, data curation, validation, visualization, writing (original draft, review and editing); Victor H. R. Souza for conceptualization, formal analysis funding acquisition, investigation, project administration, resources, validation, visualization, writing (original draft, review and editing); Elisa S. Orth for conceptualization, formal analysis funding acquisition; investigation, project administration, resources, validation, visualization, writing (original draft, review and editing).

References

1. Silva, V. B.; Campos, R. B.; Pavez, P.; Medeiros, M.; Orth, E. S.; *Chem. Rec.* **2021**, *21*, 2638. [Crossref]
2. Costanzi, S.; Koblentz, G. D.; *Nonproliferation Rev.* **2021**, *28*, 95. [Crossref]
3. Delfino, R. T.; Ribeiro, T. S.; Figueroa-Villar, J. D.; *J. Braz. Chem. Soc.* **2009**, *20*, 407. [Crossref]
4. Costanzi, S.; Machado, J. H.; Mitchell, M.; *ACS Chem. Neurosci.* **2018**, *9*, 873. [Crossref]
5. Jang, Y. J.; Kim, K.; Tsay, O. G.; Atwood, D. A.; Churchill, D. G.; *Chem. Rev.* **2015**, *115*, PR1. [Crossref]
6. Domingos, J. B.; Longhinotti, E.; Machado, V. G.; Nome, F.; *Quim. Nova* **2003**, *26*, 745. [Crossref]
7. Wanderlind, E. H.; Medeiros, M.; Souza, B. S.; Fiedler, H. D.; Nome, F.; *Rev. Virtual Quim.* **2014**, *6*, 632. [Crossref]
8. Kirby, A. J.; Nome, F.; *Acc. Chem. Res.* **2015**, *48*, 1806. [Crossref]
9. Attwood, P. V.; Piggott, M. J.; Zu, X. L.; Besant, P. G.; *Amino Acids* **2007**, *32*, 145. [Crossref]
10. Marshall, G. R.; Feng, J. A.; Kuster, D. J.; *Pept. Sci.* **2008**, *90*, 259. [Crossref]
11. Attwood, P. V.; *Biochim. Biophys. Acta, Proteins Proteomics* **2013**, *1834*, 470. [Crossref]
12. Raushel, F. M.; Holden, H. M.; *Adv. Enzymol. Relat. Areas Mol. Biol.* **2000**, *74*, 51. [Crossref]
13. Besant, P. G.; Attwood, P. V.; *Biochim. Biophys. Acta, Proteins Proteomics* **2005**, *1754*, 281. [Crossref]
14. Silva, V. B.; Orth, E. S.; *Quim. Nova* **2021**, *44*, 318. [Crossref]
15. Giusti, L. A.; Medeiros, M.; Ferreira, N. L.; Mora, J. R.; Fiedler, H. D.; *J. Phys. Org. Chem.* **2014**, *27*, 297. [Crossref]
16. Leopoldino, E. C.; Pinheiro, G.; Alves, R. J.; Gerola, A.; Souza, B. S.; *Mater. Today Commun.* **2021**, *26*, 101904. [Crossref]
17. Ferreira, J. G. L.; Takarada, W. H.; Orth, E. S.; *J. Hazard. Mater.* **2022**, *427*, 127885. [Crossref]
18. Hostert, L.; Blaskievicz, S. F.; Fonsaca, J. E.; Domingues, S. H.; Zarbin, A. J.; Orth, E. S.; *J. Catal.* **2017**, *356*, 75. [Crossref]
19. Silva, V. B.; Santos, Y. H.; Hellinger, R.; Mansour, S.; Delaune, A.; Legros, J.; Zinoviev, S.; Nogueira, E. S.; Orth, E. S.; *Green Chem.* **2022**, *24*, 585. [Crossref]
20. Breslow, R.; Anslyn, E.; *J. Am. Chem. Soc.* **1989**, *111*, 5972. [Crossref]
21. Wanderlind, E. H.; Liz, D. G.; Gerola, A. P.; Affeldt, R. F.; Nascimento, V.; Bretanha, L. C.; Montecinos, R.; Garcia-Rio, L.; Fiedler, H. D.; Nome, F.; *ACS Catal.* **2018**, *8*, 3343. [Crossref]
22. Brisebois, P.; Siaj, M.; *J. Mater. Chem. C* **2020**, *8*, 1517. [Crossref]
23. Kuila, T.; Bose, S.; Mishra, A. K.; Khanra, P.; Kim, N. H.; Lee, J. H.; *Prog. Mater. Sci.* **2012**, *57*, 1061. [Crossref]
24. Georgakilas, V.; Otyepka, M.; Bourlinos, A. B.; Chandra, V.; Kim, N.; Kemp, K. C.; Hobza, P.; Zboril, R.; Kim, K. S.; *Chem. Rev.* **2012**, *112*, 6156. [Crossref]
25. Martin-Gullon, I.; Perez, J. M.; Domene, D.; Salgado-Casanova, A. J.; Radovic, L. R. J. C.; *Carbon* **2020**, *158*, 406. [Crossref]
26. Kasprzak, A.; Zuchowska, A.; Poplawska, M.; *Beilstein J. Org. Chem.* **2018**, *14*, 2018. [Crossref]
27. Hostert, L.; Zarbin, A. J.; Orth, E. S.; *JPhys. Mater.* **2020**, *3*, 034003. [Crossref]
28. Orth, E. S.; Fonsaca, J. E. S.; Domingues, S. H.; Mehl, H.; Oliveira, M. M.; Zarbin, A. J. G.; *Carbon* **2013**, *61*, 543. [Crossref]
29. Wang, H. F.; Tang, C.; Zhang, Q.; *Nano Today* **2019**, *25*, 27. [Crossref]
30. Luo, J.; Jang, H. D.; Sun, T.; Xiao, L.; He, Z.; Katsoulidis, A. P.; Kanatzidis, M. G.; Gibson, J. M.; Huang, J.; *ACS Nano* **2011**, *5*, 8943. [Crossref]
31. Deng, S.; Berry, V.; *Mater. Today* **2016**, *19*, 197. [Crossref]
32. Luo, J.; Jang, H. D.; Huang, J.; *ACS Nano* **2013**, *7*, 1464. [Crossref]
33. Fu, H.; Huang, J.; Gray, K.; *Carbon* **2021**, *183*, 958. [Crossref]
34. Yuan, R.; Chen, W.; Zhang, J.; Zhang, L.; Ren, H.; Miao, T.; Wang, Z.; Zhan, K.; Zhu, M.; Zhao, B.; *Dalton Trans.* **2022**, *51*, 4491. [Crossref]

35. Nonaka, L. H.; Almeida, T. S. D.; Aquino, C. B.; Domingues, S. H.; Salvatierra, R. V.; Souza, V. H. R.; *ACS Appl. Nano Mater.* **2020**, *3*, 4859. [Crossref]
36. Tang, Z.; Li, X.; Sun, T.; Shen, S.; Huixin, X.; Yang, J.; *Microporous Mesoporous Mater.* **2018**, *272*, 40. [Crossref]
37. Lee, C.; Jo, E. H.; Kim, S. K.; Choi, J. H.; Chang, H.; Jang, H. D.; *Carbon* **2017**, *115*, 331. [Crossref]
38. Haddad, K.; Abokifa, A.; An, S.; Lee, J.; Raman, B.; Biswas, P.; Fortner, J. D.; *J. Mater. Chem. A* **2023**, *11*, 447. [Crossref]
39. Alencar, L. M.; Silva, A. W. B. N.; Trindade, M. A. G.; Salvatierra, R. V.; Martins, C. A.; Souza, V. H. R.; *Sens. Actuators, B* **2022**, *360*, 131649. [Crossref]
40. Boruah, P. K.; Borthakur, P.; Neog, G.; Le Ouay, B.; Afzal, N. U.; Manna, P.; Das, M. R.; *ACS Appl. Nano Mater.* **2023**, *6*, 1667. [Crossref]
41. Luo, J.; Zhao, X.; Wu, J.; Jang, H. D.; Kung, H. H.; Huang, J.; *J. Phys. Chem. Lett.* **2012**, *3*, 1824. [Crossref]
42. Liu, S.; Wang, A.; Li, Q.; Wu, J.; Chiou, K.; Huang, J.; Luo, J.; *Joule* **2018**, *2*, 184. [Crossref]
43. Lin, Y.; Ren, J.; Qu, X.; *Acc. Chem. Res.* **2014**, *47*, 1097. [Crossref]
44. Campisciano, V.; Gruttadauria, M.; Giacalone, F.; *ChemCatChem* **2019**, *11*, 90. [Crossref]
45. Domingues, S. H.; Salvatierra, R. V.; Oliveira, M. M.; Zarbin, A. J. G.; *Chem. Commun.* **2011**, *47*, 2592. [Crossref]
46. Santos, Y. H.; Martinez, A. H. G.; Veiga, A. G.; Rocco, M. L. M.; Zarbin, A. J. G.; Orth, E. S.; *ChemCatChem* **2024**, *16*, e202301440. [Crossref]
47. Santos, Y. H.; Martinez, A. H. G.; Veiga, A. G.; Rocco, M. L. M.; Zarbin, A. J. G.; Orth, E. S.; *ACS Appl. Nano Mater.* **2022**, *5*, 6001. [Crossref]
48. Chen, D.; Liu, X.; Nie, H.; *J. Colloid Interface Sci.* **2018**, *530*, 46. [Crossref]
49. Acik, M.; Lee, G.; Mattevi, C.; Pirkle, A.; Wallace, R. M.; Chhowalla, M.; Cho, K.; Chabal, Y.; *J. Phys. Chem. C* **2011**, *115*, 19761. [Crossref]
50. Ţucureanu, V.; Matei, A.; Avram, A. M.; *Crit. Rev. Anal. Chem.* **2016**, *46*, 502. [Crossref]
51. Surabhi; Sah, D.; Shabir, J.; Gupta, P.; Mozumdar, S.; *ACS Appl. Nano Mater.* **2022**, *5*, 5776. [Crossref]
52. Gonçalves, D. A.; Alencar, L. M.; Anjos, J. P. B.; Orth, E. S.; Souza, V. H. R.; *Mater. Today Commun.* **2023**, *36*, 106746. [Crossref]
53. Blaskievicz, S. F.; Endo, W. G.; Zarbin, A. J. G.; Orth, E. S.; *Appl. Catal., B* **2020**, *264*, 118496. [Crossref]
54. Mao, S.; Wen, Z.; Huang, T.; Hou, Y.; Chen, J.; *Energy Environ. Sci.* **2014**, *7*, 609. [Crossref]
55. Zhao, J.; Tang, Z.; Qiu, Y.; Gao, X.; Wan, J.; Bi, W.; Shen, S.; Yang, J.; *J. Mater. Sci.* **2019**, *54*, 8108. [Crossref]
56. El Rouby, W. M. A.; *RSC Adv.* **2015**, *5*, 66767. [Crossref]

Submitted: January 24, 2024
Published online: April 23, 2024